

A Multidomain Adhesion Protein Family Expressed in *Plasmodium falciparum* Is Essential for Transmission to the Mosquito

Gabriele Pradel,¹ Karen Hayton,² L. Aravind,³
Lakshminarayan M. Iyer,³ Mitchell S. Abrahamsen,⁴
Annemarie Bonawitz,¹ Cesar Mejia,¹ and Thomas J. Templeton¹

¹Department of Microbiology and Immunology, Weill Medical College of Cornell University, New York, NY 10021

²Laboratory of Malaria and Vector Research, National Institute of Allergy and Infectious Diseases, and ³National Center for Biotechnology Information, National Library of Medicine, National Institutes of Health, Bethesda, MD 20892

⁴Biomedical Genomics Center and Department of Veterinary Pathobiology, University of Minnesota, St. Paul, MN 55108

Abstract

The recent sequencing of several apicomplexan genomes has provided the opportunity to characterize novel antigens essential for the parasite life cycle that might lead to the development of new diagnostic and therapeutic markers. Here we have screened the *Plasmodium falciparum* genome sequence for genes encoding extracellular multidomain putative adhesive proteins. Three of these identified genes, named *PfCCp1*, *PfCCp2*, and *PfCCp3*, have multiple adhesive modules including a common *Limulus* coagulation factor C domain also found in two additional *Plasmodium* genes. Orthologues were identified in the *Cryptosporidium parvum* genome sequence, indicating an evolutionary conserved function. Transcript and protein expression analysis shows sexual stage-specific expression of *PfCCp1*, *PfCCp2*, and *PfCCp3*, and cellular localization studies revealed plasma membrane-associated expression in mature gametocytes. During gametogenesis, *PfCCps* are released and localize surrounding complexes of newly emerged microgametes and macrogametes. *PfCCp* expression markedly decreased after formation of zygotes. To begin to address *PfCCp* function, the *PfCCp2* and *PfCCp3* gene loci were disrupted by homologous recombination, resulting in parasites capable of forming oocyst sporozoites but blocked in the salivary gland transition. Our results describe members of a conserved apicomplexan protein family expressed in sexual stage *Plasmodium* parasites that may represent candidates for subunits of a transmission-blocking vaccine.

Key words: malaria • gametocyte • gamete • *Anopheles* • sporozoite

Introduction

The malaria parasite *Plasmodium* is a major cause of global human morbidity and mortality, whereas other apicomplexan parasites like *Cryptosporidium parvum* and *Toxoplasma gondii* are important opportunistic pathogens in immunocompromised individuals such as AIDS patients. An important aspect of apicomplexan biology is the molecular basis for their interaction with target cells, extracellular matrices, and hemo-lymphatic fluids of their animal hosts. Due to

their extracellular localization, surface proteins proposed to be involved in these processes are likely accessible by host-immune sera and are therefore vaccine candidates stimulating antibody-mediated protection. Recent methodologies to identify extracellular proteins as research targets include “postgenomic” techniques such as genome sequence annotation, microarray screening, and proteomics. Of particular importance, completion of *Plasmodium* sp. genome sequences (1, 2) and the imminent completion of additional apicomplexan genomes have provided an unprecedented opportunity

The online version of this article contains supplemental material.

Address correspondence to Thomas J. Templeton, Department of Microbiology and Immunology, Weill Medical College of Cornell University, 1300 York Avenue, Box 62, New York, NY 10021. Phone: (212) 746-4467; Fax: (212) 746-4028; email: tjt2001@med.cornell.edu

Abbreviations used in this paper: CS, circumsporozoite; ER, endoplasmic reticulum; IFA, immunofluorescence; LCCL, *Limulus* coagulation factor C; MBP, maltose-binding protein; SR, scavenger receptor.

to identify novel antigens as prospective vaccine targets for study, as well as underpin a better understanding of *Plasmodium* and apicomplexan biology.

In the search for novel extracellular proteins as prospective vaccine candidates, we have exhaustively identified genes encoding extracellular proteins through genome sequence analysis of *Plasmodium* sp. and the recently completed *C. parvum* genome sequence, as well as whole genome comparison of the resulting catalogs of extracellular proteins (unpublished data). Here we describe a select subset of sexual stage-specific genes in the human malaria parasite, *P. falciparum*, that are striking for multidomain architectures composed of animal- and bacterial-like putative adhesive domains. Orthologues are present in the *C. parvum* genome sequence, indicating a cellular function likely conserved across the apicomplexan clade. These proteins are grouped as a family based upon a common *Limulus* coagulation factor C (LCCL) domain and are accordingly named CCp proteins, of which five genes are present in the *P. falciparum* genome sequence (*PfCCps*). One of these proteins, herein referred to as *PfCCp3*, was recently described as PSLAP in *P. falciparum* (3) and *PbSR* in *Plasmodium berghei* (4). These two studies presented, in part, contradictory conclusions regarding protein expression. Although PSLAP was shown to be expressed in the gametocyte stages, *PbSR* protein expression was described as sporozoite stage-specific and *PbSR*-targeted gene disruption led to inhibited sporozoite formation. In this study, we characterize three *P. falciparum* members of the LCCL family, *PfCCp1*, *PfCCp2*, and *PfCCp3*/PSLAP, based upon their striking multiadhesion domain structures. We show that *PfCCp1*, *PfCCp2*, and *PfCCp3* are specifically expressed in gametocytes and released during gametogenesis. Disruption of the *PfCCp2* or *PfCCp3* gene loci via homologous recombination leads to a blockage in the *P. falciparum* sporozoite midgut to salivary gland transition. We suggest that the *PfCCp* protein family serves a role in multiple mosquito parasite stages and has an essential role in transmission to the mosquito, thus warranting further study as transmission-blocking vaccine candidates.

Materials and Methods

Apicomplexan Genome Sequence Analysis. *CCp* genes were identified via screening of complete *Plasmodium* sp. and *C. parvum* genome sequence databases using the gapped version of the BLAST programs (BLASTPGP and TBLASTNGP, with both the single pass and the recently incorporated multipass profile option for translating searches of nucleotide databases). Sequence profile searches were performed using the PSI-BLAST program (5). Profiles were saved using the -C option and retrieved using the -R option. Complete domain architectures of identified proteins were determined by screening the nonredundant protein sequence database, the Expressed Sequence Tags database (National Center for Biotechnology Information), and the individual protein sequence databases of completely and partially sequenced genomes (accessible at http://www.ncbi.nlm.nih.gov/Microb_blast/unfinishedgenome.html). Multiple alignments of amino acid sequences were generated using a combination of

PSI-BLAST and T-Coffee (6). Secondary structure predictions were produced using the PHD program (7), with multiple alignments of individual protein families used as queries. Preliminary phylogenetic trees were constructed using the neighbor-joining algorithm as implemented in the Mega2 package (8), or the least squares methods as implemented in the FITCH program of the PHYLIP package (9). These trees were used to obtain the maximum likelihood tree using the PROTML program of the MOLPHY package. The statistical significance of the trees was assessed using the relative estimates of the logarithmic likelihood (RELL) bootstrap values (10). Signal peptides in protein sequences were predicted using the SignalP program (11) and membrane topologies were predicted using the TMHMM2 package (12).

Parasite Culture and Mosquito Membrane Feeds. Asexual and mature gametocyte NF54 isolate *P. falciparum* parasites were cultivated in vitro as described previously (13). Gametogenesis was induced by incubating mature gametocyte cultures in human serum for 5–30 min at room temperature as described previously (14). Zygote formation was achieved by incubation of emerged gametes in human serum overnight at room temperature. Zygotes and gametocytes were enriched via centrifugation over 6/11/16% Accudenz gradients and parasites were collected at gradient interfaces. Mosquito stages (retorts, ookinetes, oocysts, and salivary gland sporozoites) were obtained after membrane feeds of *Anopheles freeborni* mosquitoes on blood containing mature gametocytes as described previously (15). Retort and mature ookinetes were obtained by harvesting midgut bloodmeals 24 h after feeding. Oocysts were isolated from mosquito midguts 12 d after feeding. Sporozoite preparations were enriched by centrifugation from pooled, homogenized infected salivary glands isolated 18–20 d after feeding. To determine the efficiency of mosquito transmission, WT NF54- or *PfCCp*-KO-targeted gene-disruptant isolates were membrane fed to mosquitoes and oocyst numbers were assayed in mercurochrome-stained midguts 8–12 d after feeding. Similarly, the presence of salivary gland sporozoites was assayed 18–21 d after feeding.

Recombinant Protein Production and Derivation of Mouse Antisera. Recombinant protein construct designs were guided by domain architecture determinations for *PfCCp1* (sequence data are available from GenBank/EMBL/DDBJ under accession no. NP_702612.1), *PfCCp2* (GenBank/EMBL/DDBJ under accession no. NP_702421.1), and *PfCCp3* (GenBank/EMBL/DDBJ under accession no. NP_701955) amino acid sequences. For each *PfCCp* gene, recombinant protein was produced corresponding to discrete domains, such as the LCCL domain (*PfCCp1*), the discoidin domain (*PfCCp2*), and the two tandem scavenger receptor (SR) domains (*PfCCp3*). Recombinant protein was expressed as fusions downstream of the maltose-binding protein (MBP) using the pMAL expression vector (New England Biolabs, Inc.). All constructs were generated by ligation of PCR products corresponding to discrete *PfCCp* domains amplified from 3D7 (clone of NF54 isolate) *P. falciparum* gametocyte stage cDNA. Recombinant protein was purified from bacterial extracts by sequential steps of amylose affinity (New England Biolabs, Inc.) and ion exchange chromatography (Source 15Q resin using an AKTA Prime chromatography system; Amersham Biosciences). 6-wk-old female CAF1 mice were immunized with 30–100 µg recombinant protein emulsified in Freund's complete adjuvant followed by two boosts at 3-wk intervals in Freund's incomplete adjuvant. Immune sera were collected 10 d after the third immunization. All antisera recognized cognate recombinant protein via Western blot analysis. Sera from prebleed and MBP protein alone-immunized mice served as controls for all antibody reagent studies. As a

second source of antisera for double labeling experiments, anti-peptide sera, directed against a *PfCCp2* peptide sequence within the discoidin domain (CDKIKDTDDARDKYF), was produced in rabbits immunized with KLH-conjugated material produced using a maleimide-activated KLH kit (Pierce Chemical Co.). Immunizations of two rabbits were performed by Spring Valley Laboratories, Inc.

Western Blot Analysis. Mixed asexual stage parasites and Acaudenz gradient-enriched gametocytes were saponin lysed and suspended in PBS and SDS-PAGE loading buffer. Salivary glands infected with sporozoites were dissected from *An. freeborni* mosquitoes and suspended in SDS-PAGE loading buffer. Parasite proteins were separated by electrophoresis (Novex PAGE system; Invitrogen) and transferred to Hybond ECL nitrocellulose membrane (Amersham Biosciences) according to the manufacturer's instructions. Membranes were blocked for nonspecific binding in Tris-buffered saline containing 3% skim milk and incubated for 2 h at room temperature with mouse immune sera specific to *PfCCps*, mouse mAb 2A10 recognizing the sporozoite surface circumsporozoite (CS) protein (16), MBP fusion partner protein control, or, as a control for loading, mouse sera recognizing the abundant *P. falciparum* endoplasmic reticulum (ER) protein, *Pf39* (17, 18). After washing, membranes were incubated for 1 h at room temperature with an alkaline phosphatase-conjugated secondary antibody (Kirkegaard & Perry Laboratories, Inc.) and developed in NBT/BCIP solution (Sigma-Aldrich) for 5–15 min.

Immunofluorescence (IFA) and Confocal Laser Scanning Microscopy. Parasite preparations for IFA microscopy included NF54 isolate-mixed asexual stages, mature gametocytes, emerging gametes, mosquito midgut blood smears 24 h after feeding, midgut oocysts 12 d after feeding, or salivary gland sporozoite smears 18 d after feeding. Preparations were either fixed for 4 d in 4% paraformaldehyde in PBS at 4°C or were air dried on slides and fixed for 10 min in –80°C cold methanol. For membrane permeabilization and blocking of nonspecific binding, fixed cells were incubated in 0.02% saponin, 0.5% BSA, and 1% neutral goat serum (Sigma-Aldrich) in PBS twice for 30 min each. Preparations were then incubated for 2 h at 37°C with either mouse immune sera recognizing specific *PfCCps*, mouse mAb 2A10 recognizing the CS protein, rabbit anti- α -tubulin II serum (American Type Culture Collection [ATCC]; reference 19), or rabbit immune serum recognizing *Pf25* (ATCC; references 20 and 21). Binding of primary antibody was visualized using fluorescence-conjugated goat anti-mouse or goat anti-rabbit secondary antibodies (Alexa Fluor 488 or Alexa Fluor 594; Molecular Probes). To highlight unlabeled parasites, selected specimens were further incubated with the nuclear dye TOTO-3 (Molecular Probes) for 30 min at 37°C. Paraformaldehyde-fixed samples were embedded in 1% agarose in PBS, coated onto slides, and air dried. In selected preparations, those not requiring Alexa 594 conjugation, counterstaining was performed using 0.05% Evans Blue (Sigma-Aldrich) in PBS. Labeled specimens were examined by confocal laser scan microscopy using a Zeiss LSM 510, and digital images were processed using Adobe Photoshop 6.0 software.

Electron Microscopy. For preembedding immunolabeling, mixed asexual and gametocyte stages were fixed in 4% paraformaldehyde in PBS for 4 d at 4°C. Cells were blocked in 0.02% saponin, 0.5% BSA, and 5% neutral goat serum (Sigma-Aldrich) in PBS for twice for 30 min each, and then incubated for 2 h at 37°C with mouse immune sera against *PfCCps*, followed by incubation with a goat anti-mouse secondary antibody conjugated with either 10 nm gold (Amersham Biosciences) or alkaline phosphatase. Alkaline phosphatase labeling was detected by incubating

cells in BCIP/NBT solution for 20 min. Cells were then embedded in agar, fixed in 1% glutaraldehyde and 4% paraformaldehyde in PBS for 1 d at 4°C, postfixed in 1% osmium tetroxide in PBS for 1 h, and dehydrated in successive washes at increasing concentrations of ethanol. Specimens were embedded in Epon (Electron Microscopy Sciences) at 60°C for 2 d. Photographs were taken with a JEOL 100CX-II transmission electron microscope and scanned images were processed using Adobe Photoshop 6.0 software. For the morphological examination of *PfCCp2*-targeted gene-disruptant (*PfCCp2*-KO) oocysts, infected mosquito midguts were fixed in 1% glutaraldehyde and 4% paraformaldehyde in PBS for 2 d, and postfixed in 1% osmium tetroxide and 1.5% $K_3Fe(CN)_6$ in PBS for 2 h, followed by incubation in 0.5% uranyl acetate for 1 h. Midguts were dehydrated in ethanol and embedded in Epon as described above.

Generation of Gene-disruptant Parasites. A *PfCCp2* KO construct, *pPfCCp2*-KO, was designed such that after homologous integration a “pseudo-diploid” locus is generated in which the first copy of the disrupted gene is truncated and possesses an in-frame stop codon at the 3' end, whereas the second copy is truncated at the 5' end and lacks a start methionine, a signal peptide sequence, and the start of the coding region. The disruption construct contained a 523-bp amino-terminal region segment of *PfCCp2* that was PCR amplified from NF54 *P. falciparum* genomic DNA template using gene-specific 5' primer 5'-TAGCGGCCGCACCCTAATGGCACC GAAT-3' and 3' primer 5'-ATGCGGCCGCTTAAGGAGA ACTAGGTAACGC-3'. Each primer introduced a NotI restriction site (underlined) to facilitate ligation of restriction enzyme-digested PCR product into a NotI-cut pDT-Tg23 vector (22, 23). The *PfCCp3* KO construct, *pPfCCp3*-KO, was similarly designed and contained a 565-bp amino-terminal region segment that was amplified from NF54 WT DNA using gene-specific 5' primer 5'-TAGCGGCCGCAGCTGGATAGGTGCTCCT-3' and 3' primer 5'-ATGCGGCCGCTTATACACAAACGGTACCCCA-3'. The resulting constructs were loaded into uninfected erythrocytes via electroporation, and the erythrocytes were then inoculated with NF54 isolate parasites (24). At the time of the first parasite passage, this process was repeated such that the parasite cultures were diluted into freshly electroporated erythrocytes. After 3 d, 10 mM pyrimethamine drug pressure was initiated to select for *TgDHFR* expression in parasites that have taken up and retained plasmid. After ~90 d of pyrimethamine drug pressure a plasmid-integrant population predominated and the presence of homologous gene disruptants was demonstrated by a diagnostic PCR assay of a disrupted locus (described in Fig. 7). At this time, transformed parasite clones were isolated by dilution cloning in microtiter plates using the Malstat reagent assay (25) as an indicator of parasite-positive wells. Homologous recombination in clonal isolates was confirmed by the above PCR assay and in select isolates was further confirmed by Southern blot analysis (see Supplemental Materials and Methods, which is available at <http://www.jem.org/cgi/content/full/jem.20031274/DC1>).

Online Supplemental Material. Methods regarding RNA isolation, transcript level analysis, and Southern Blot analysis are described in Supplemental Material and Methods. Fig. S1 demonstrates gametocyte stage-specific transcript expression of the six genes encoding the multidomain adhesion proteins *PfCCp1* through *PfCCp5* and *PfFNPA*. Fig. S2 shows analysis of *PfCCp2*- and *PfCCp3*-targeted gene disruptions by Southern blotting (Fig. S2, A and C), and the resulting loss of *PfCCp2* and *PfCCp3* protein expression analyzed by Western blotting (Fig. S2, B and D). Supplemental Materials and Methods and Figs. S1 and

Results

Domain Structure of the LCCL Domain-containing Protein Family. Annotation of apicomplexan genomes reveals numerous genes encoding extracellular proteins having multidomain architectures reminiscent of, but in no case identical to, extracellular proteins found in multicellular organisms. We have recently conducted a whole genome comparison of *P. falciparum* and *C. parvum* genome sequences (unpublished data) and have exhaustively identified genes remarkable for multidomain “animal-like” architectures, in some instances conserved in orthologues present across the apicomplexan clade. Five of these proteins exhibit striking multiple adhesion modules and are herein grouped based upon the presence of a shared LCCL-like domain. The *P. falciparum* versions were accordingly termed *PfCCp1* through *PfCCp5* (see schematic in Fig. 1). *PCCp3* has recently been variously described as *PSLAP* in *P. falciparum* and as *PbSR* in *P. berghei* to highlight the presence of tandem SR-like domains in addition to four copies of the LCCL domain (3, 4). *CCp* orthologues are conserved in *C. parvum*, as well as across the *Plasmodium* clade, with versions identified in the *Plasmodium yoelii* genome sequence and isolation of *P. berghei* versions, including *PbCCp2* (sequence data are available from GenBank/EMBL/DDBJ under accession no. AF491294) and *PbCCp3* (*PbSR*; GenBank/EMBL/DDBJ under accession no. AY034780). All *PCCp* genes possess signal peptide

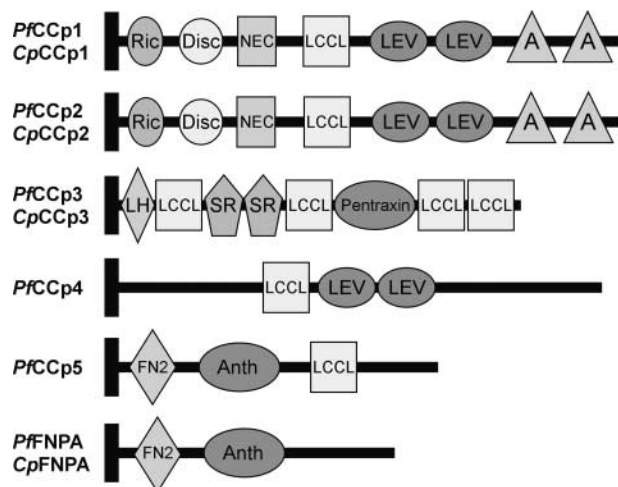


Figure 1. Domain organization of the apicomplexan LCCL domain-containing gene family in *P. falciparum* (designated with prefix *Pf*) and orthologues present in *C. parvum* (designated with prefix *Cp*). All proteins have a signal peptide sequence represented by a black box at the beginning of the architectures. Ric, ricin domain; Disc, discoidin domain; A, ApicA domain; Anth, anthrax toxin NH₂-terminal region domain; FN2, fibronectin type II domain; LCCL, Limulus coagulation factor C domain; Lev, levanase domain; LH, lipoxigenase domain; NEC, neurexins and collagens domain; SR, scavenger receptor domain.

sequences as predicted by the SignalP algorithm (11). Transmembrane domains were not identified in *PfCCp1* through *PfCCp5*, as predicted by the TMHMM2 program (12), nor are GPI anchor signal sequences present. Thus, given the predicted signal peptides, lack of ER retention or other organelle trafficking signals and the presence of disulfide bond containing extracellular adhesive domains combine to suggest that all *PCCp* proteins are secreted and serve extracellular functions, perhaps in parasite–parasite or parasite–host interactions.

PfCCp1 and *PfCCp2* have similar architectures and are paralogs arising via relatively recent gene duplication after domain accretion. *C. parvum* also has paralogs, *CpCCp1* and *CpCCp2*, and thus the gene duplication event likely occurred before the divergence of the apicomplexan genera. Within *PfCCp1* and *PfCCp2*, we identified three predicted polysaccharide-binding domains, namely ricin, discoidin, and levanase-type lectin domains (26, 27). COOH terminal to these modules are two copies of an apicomplexan-specific cysteine-rich module (herein termed ApicA) that has not been identified in any other gene. Between the discoidin and levanase lectin domains there are two distinct cysteine-rich modules, the described animal- and fungal-specific LCCL domain (28), and a novel module, termed NEC, which appears in a wide range of animal proteins such as neurexins (29), fibrillar collagen α globular domain (30) from vertebrates and sponges, and the fibrinogen family of proteins (31). The NEC domain has not been identified previously as a distinct module because in all the animal instances it occurs in combination with other cysteine-rich segments. This has resulted in it being considered a portion of several other distinct modules such as the fibrinogen globular domain (31, 32) or the fibrillar collagen α COOH-terminal globular domain (30). We term this module the NEC domain after neurexins (29) and collagens, the two ancient animal surface proteins in which they are represented. This is the first instance in which the NEC domain occurs in a stand alone form and is consistent with it forming a distinct NH₂-terminal folding α - β unit stabilized by a cysteine bridge in the fibrinogen crystal structure (Fig. 2). The structure of this domain reveals a distinct cleft that is likely to function as a binding pocket (32). Several animal proteins functioning as lectins contain the NEC domain, such as ficolin and intelectin (33, 34), suggesting that it probably represents a fourth sugar-binding domain in the *PfCCp* proteins. Phylogenetic analysis suggests that the levanase lectin and discoidin domains group closer to the bacterial forms as opposed to those from other organisms (Fig. 3 A), whereas the NEC domain groups with animal affinity (Fig. 3 B). Thus, the extracellular adhesion modules can be attributed to multiple distinct heritages, those originally derived in bacteria or animals and laterally transferred to Apicomplexa, and those “invented” within the lineage leading to the Apicomplexa.

The domain architecture of *PfCCp3* (*PSLAP*/*PbSR*) has been recently described in detail (3, 4) and contains, in addition to four LCCL domains, a tandem repeat of an SR-

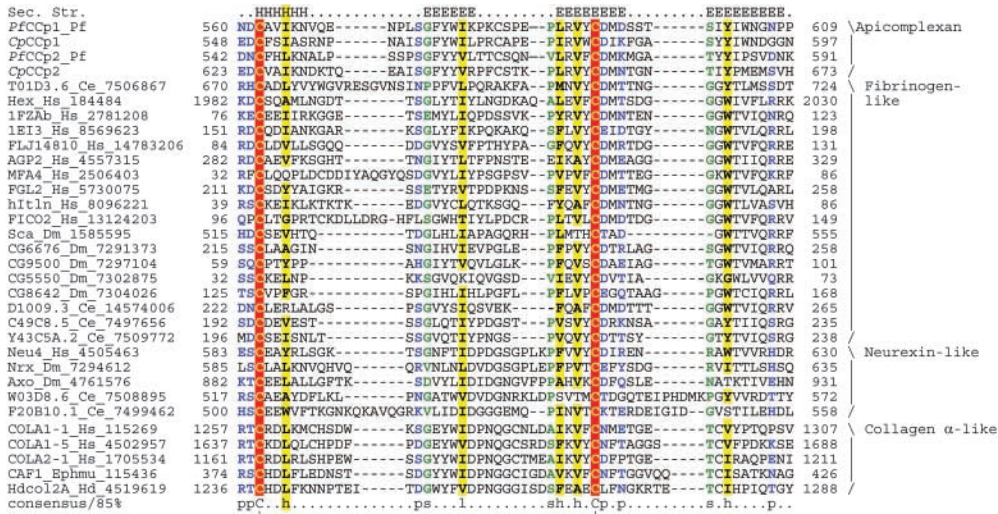


Figure 2. Multiple sequence alignment of the NEC domain. Proteins are designated by their gene name abbreviations and GenBank identifier numbers. The apicomplexan proteins are represented by their gene names only. The coloring reflects 85% consensus. The consensus abbreviations and coloring scheme are as follows: h, hydrophobic residues (LIYFMWACV) and l, aliphatic (LIAV) residues shaded yellow; c, charged (KERDH) residues and p, polar (STEDRKHNQ) residues colored blue; s, small (SAGDNPVT) residues colored green; C, conserved disulfide bonding cysteines are shaded red. In the secondary structure annotation, E represents a residue in a strand (extended) and H represents a residue in a helix. Species abbreviations are as follows: Ce, *Caenorhabditis elegans*; Dm, *Drosophila melanogaster*; Ephmu, *Ephydatia muelleri*; Hd, *Haliotis discus*; Hs, *Homo sapiens*; Pf, *Plasmodium falciparum*.

like domain, an LH2 domain with a predicted role in lipid binding, and a region similar to pentraxin. Pentraxin and the SR domain have thus far been found only in the extracellular proteins of animals other than apicomplexans. *PfCCp4* possesses a single LCCL domain followed by tandem levanase domains, plus additional anonymous cysteine-rich globular domains within the amino-terminal region. *PfCCp5* encodes a region at the amino terminus that

is similar to a domain found within fibronectin (FN2), followed by a domain similar to the amino-terminal region of anthrax-protective antigen that may bind host cell polysaccharides, and a single LCCL domain near the carboxy terminus. An additional *P. falciparum* gene, herein named *PfFNPA*, is similar to *PfCCp5* in overall architecture but lacks an LCCL domain. Given that *PfFNPA* has an apparent *C. parvum* orthologue (Fig. 1), the two genes are likely

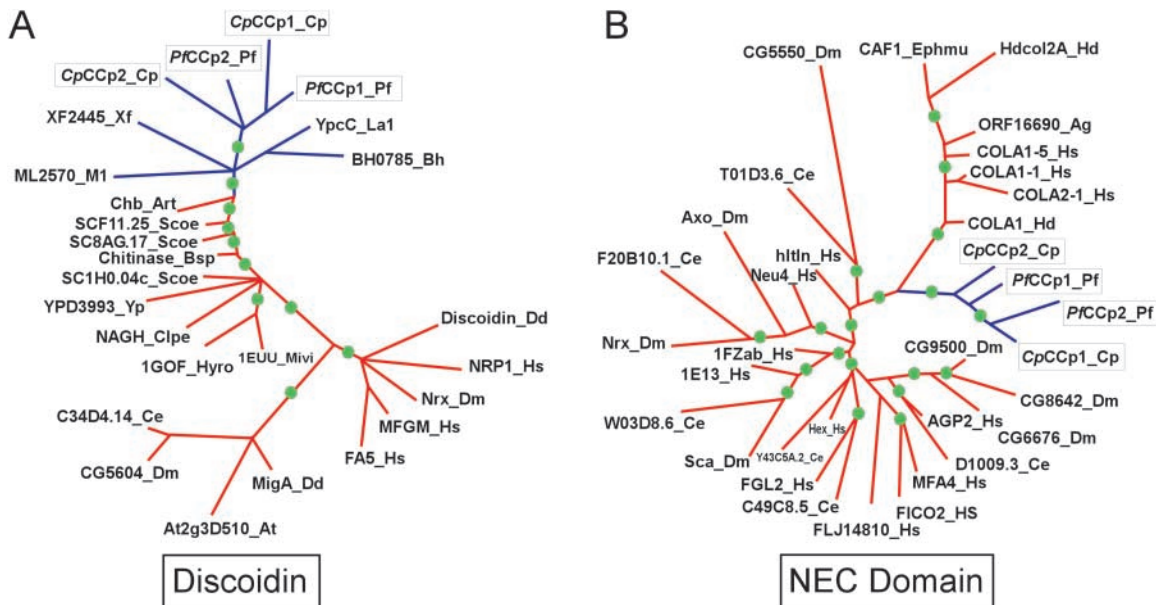


Figure 3. Phylogenetic trees showing affinity of apicomplexan versions to bacterial discoidin (A) and animal NEC (B) domains. Principal nodes supported by bootstrap values of >65% are shown with a filled green circle. Clades containing apicomplexan sequences are colored blue and apicomplexan sequences are boxed. Genes are designated by their gene names and the abbreviated source species names are as follows: Art, *Arthrobacter spp.*; At, *Arabidopsis thaliana*; Bh, *Bacillus halodurans*; Bsp, *Bacillus spp.* D-2; Ce, *Caenorhabditis elegans*; Clpe, *Clostridium perfringens*; Cp, *Cryptosporidium parvum*; Dd, *Dictyostelium discoidium*; Dm, *Drosophila melanogaster*; Hs, *Homo sapiens*; Hyro, *Hypomyces rosellus*; Lal, *Lactococcus lactis*; Mivi, *Micromonospora viridifaciens*; Pf, *Plasmodium falciparum*; Scoe, *Streptomyces coelicolor*; Xf, *Xylella fastidiosa*; Yp, *Yersinia pestis*.

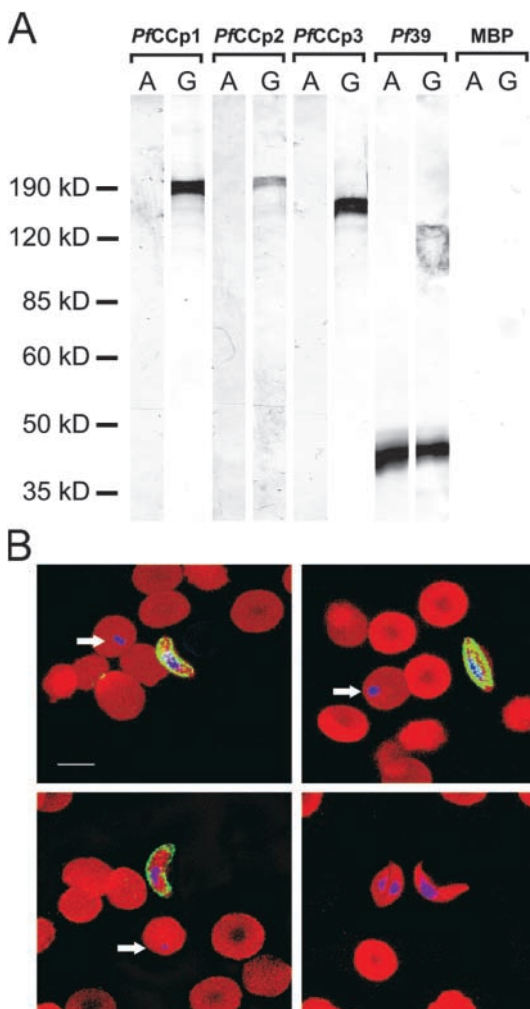


Figure 4. Membrane-associated protein expression of *PfCCps* in mature gametocytes. (A) Western blot analysis of extracts from mixed asexual (lanes A) and mature gametocyte (lanes G) stages show gametocyte-specific *PfCCp* expression. As a control for protein loading, extracts were additionally screened with mouse sera recognizing *Pf39*, an abundant ER-resident protein (lanes marked *Pf39*). Lanes marked MBP indicate lack of reactivity with mouse control sera recognizing the recombinant fusion partner MBP. (B) Indirect IFA assay using mouse sera against *PfCCp1*, *PfCCp2*, and *PfCCp3* revealed a punctate pattern associated to the parasite surface in mature gametocytes (green Alexa Fluor 488), whereas asexual stage parasites did not exhibit any labeling. Mouse sera directed against MBP shows no labeling of gametocytes. Erythrocytes were counterstained with Evans Blue (red). Arrows indicate asexual parasites visualized by TOTO-3 nuclear stain (blue). Bar, 5 μm .

to have diverged in *P. falciparum* from a common ancestor that was similar in architecture to *PfFNPA*, followed by accretion of an LCCL domain in *PfCCp5*.

Expression of *PfCCps* during the Parasite Life Cycle. Transcript expression was studied by real time RT-PCR analysis using RNA isolated from asexual and gametocyte intraerythrocytic *in vitro*-cultivated *P. falciparum* parasites. Expression was gametocyte stage specific for *PfCCp1* through *PfCCp4* and *PfFNPA*, in comparison with transcript expression controls for asexual (*AMA-1*) and gametocyte (*Pfs48/45*) stage-specific genes (Fig. S1, available

at <http://www.jem.org/cgi/content/full/jem.20031274/DC1>). *PfCCp5* showed transcript expression in asexual parasites in addition to its expression in gametocyte stages (Fig. S1). *PfCCp1*, *PfCCp2*, and *PfCCp3* were chosen for further study of life cycle expression and cellular localization due to their striking multidomain architectures and the presence of orthologues in other apicomplexans. Protein expression for *PfCCp1*, *PfCCp2*, and *PfCCp3* was shown to be gametocyte stage specific as assayed by Western blot analysis using mouse sera generated against *PfCCp1*, *PfCCp2*, and *PfCCp3* recombinant protein (Fig. 4 A). Protein bands detected in gametocyte preparations had the expected molecular weights of roughly 185 kD for *PfCCp1* and *PfCCp2*, and 150 kD for *PfCCp3*. Control mouse sera directed against the MBP recombinant protein fusion partner showed no labeling in gametocyte and asexual preparations, whereas the loading control mouse antibody *Pf39* recognized a 39-kD ER protein (17, 18) abundantly expressed in both asexual and gametocyte parasites.

Cellular localization was studied via indirect IFA confocal laser scanning microscopy and immunoelectron microscopy. For *PfCCp1*, *PfCCp2*, and *PfCCp3*, a punctate rim fluorescence pattern was observed in *P. falciparum* gametocytes, whereas asexual stage parasites did not show any labeling (Fig. 4 B). Labeling was first observed in gametocytes stage III and remained throughout maturation (unpublished data). Colocalization of the three *PfCCp* proteins was investigated using rabbit sera generated against

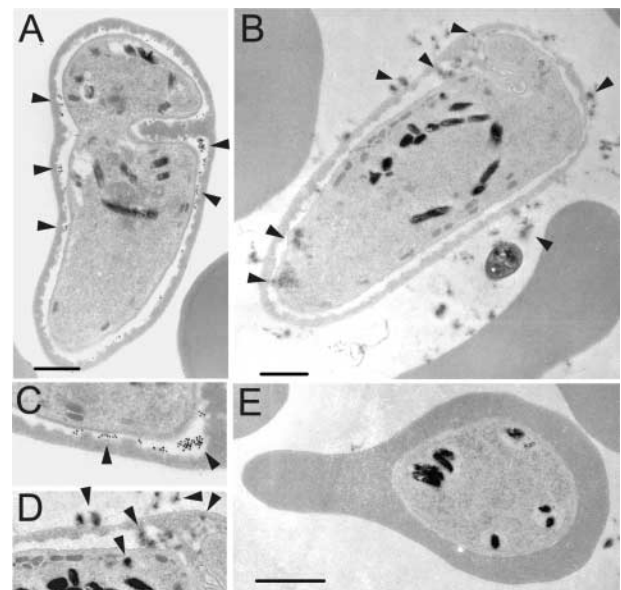


Figure 5. Ultrastructural *PfCCp1* localization associates with the parasite membrane in the parasitophorous vacuole. Immunoelectron microscopic examination using anti-*PfCCp1* primary antibody and either immunogold (A, enlarged in C) or alkaline phosphatase (B, enlarged in D) secondary labeling localize expression to the parasitophorous vacuole of mature gametocytes as well as in the gametocyte cytoplasm and attached to the outside of erythrocyte membranes. (E) No labeling was found in asexual parasites and erythrocytes (here shown for alkaline phosphatase labeling). Bars, 1 μm .

PfCCp2 peptide sequences in combination with mouse antisera against *PfCCp1* and *PfCCp3*, respectively. Experiments revealed colocalization of all three proteins at the gametocyte surface (unpublished data). Double labeling experiments, using rabbit sera recognizing α -tubulin II as a marker for microgametocytes (19), further indicated that *PfCCp* proteins are expressed in both microgametocytes and macrogametocytes (unpublished data). The ultrastructural localization of *PfCCp1* was additionally investigated by immunoelectron microscopy using two different pre-embedding labeling techniques. Immunogold labeling revealed localization of *PfCCp1* associated with the parasite surface membrane in the parasitophorous vacuole of mature gametocytes (Fig. 5, A and C). Similar results were obtained by alkaline phosphatase labeling, which results in a loose precipitation at the site of protein expression (Fig. 5, B and D). Alkaline phosphatase labeling further showed protein localization in the cytoplasm of gametocytes and attached to the outside of erythrocytes, indicating possible release of the protein. No labeling was detected in asexual parasites or erythrocytes (Fig. 5 E). We further investigated the role of *PfCCps* during gamete emergence, triggered by incubation at room temperature in the presence of human serum. Although mature gametocytes exhibited *PfCCp* labeling associated with the parasite surface (Fig. 6 A), during emergence labeling was detected outside the infected

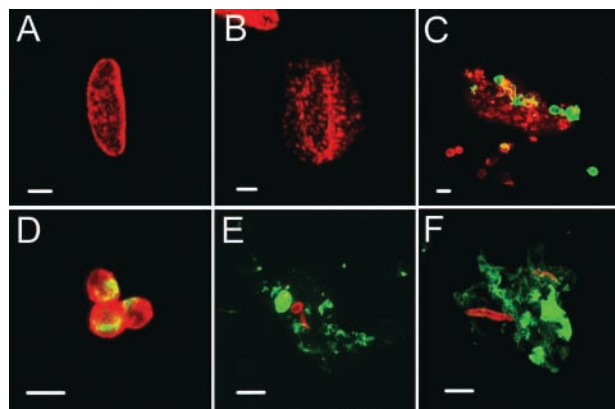


Figure 6. *PfCCps* are present within mature gametocytes and localize extracellularly after gametogenesis, but expression ceases after fertilization. (A) *PfCCp* protein labeling in mature gametocytes is associated with the parasite surface, whereas (B) *PfCCp* protein is released during the emergence of gametes from within erythrocytes. (C) *PfCCp* expression markedly decreases in emerged gametes and protein instead localizes extracellularly (red Alexa Fluor 594), adhering to complexes of emerged macrogametetes and adhering microgametes (green Alexa Fluor 488; detected with rabbit α -tubulin II antiserum). (D) Zygotes or unfertilized macrogametetes detected with rabbit *Pf*25 antiserum (red Alexa Fluor 594) exhibited a low remaining expression for *PfCCps* (green Alexa Fluor 488) 20 h after gamete emergence in vitro. Bloodmeal preparations isolated from mosquito midguts 24 h after feeding on gametocyte cultures revealed neither *PfCCp* expression (green Alexa Fluor 488) in (E) retort stages nor in (F) ookinetes (red Alexa Fluor 594, detected with *Pf*25 antiserum), whereas gamete complexes in the bloodmeal preparations still showed associated *PfCCp* labeling. Labeling shown is for *PfCCp1*. Similar results were obtained for *PfCCp2* and *PfCCp3* (not depicted). Bars, 2 μ m (A and B) and 10 μ m (C–F).

erythrocytes (Fig. 6 B). Consistent with a secreted release of *PfCCps*, we have observed that *PfCCp* expression markedly decreases in emerged gametes and protein localizes extracellularly, adhering to complexes of macrogametetes (Fig. 6 C). These complexes are readily observable in vitro due to the high gametocytemia of the parasite cultures and are formed by the inherently “sticky” macrogametetes associating with exflagellating microgametes, mature gametocytes, and erythrocytes.

PfCCp expression ceases after emergence of gametes and formation of zygotes. Double labeling using rabbit sera recognizing *Pf*25, a marker to identify unfertilized macrogametetes, zygotes, and ookinetes (20, 21), revealed a low remaining expression for *PfCCps* in zygotes 20 h after gametocyte emergence in vitro (Fig. 6 D). Bloodmeal preparations isolated from mosquito midguts 24 h after feeding on gametocyte cultures did not show *PfCCp* protein expression in retort stages (Fig. 6 E) nor in ookinetes (Fig. 6 F). Macrogamete complexes present in the bloodmeal retained *PfCCp* labeling, suggesting that released *PfCCp* proteins persist within an extracellular matrix surrounding the macrogamete aggregates. *PfCCp* expression was not found in mature oocysts 12 d after feeding, nor in midgut or salivary gland sporozoites, using mAb 2A10 recognizing *P. falciparum* CS protein (16) as a positive immunolabeling control (unpublished data). Reexpression of *PfCCp* proteins in salivary gland sporozoites was additionally investigated by Western blot analysis. No labeling for *PfCCp1*, *PfCCp2*, or *PfCCp3* was detected in a sporozoite lysate, whereas screening with mAb 2A10 detected two expected protein bands of \sim 45–50-kD molecular weights (unpublished data).

Disruption of the *PfCCp2* and *PfCCp3* Gene Loci and Characterization of the Disruptant Phenotype. The *PfCCp2* and *PfCCp3* gene loci were independently disrupted to begin characterizations of *PfCCp* family function, as well as to provide confirmations of life cycle stage of protein expression. Fig. 7 shows a schematic of the targeted gene KO construct, *pPfCCp2-KO*, designed to generate a disrupted pseudo-diploid locus after homologous integration. A *pPfCCp3-KO* construct was designed similarly for *PfCCp3*-targeted disruption. After transformation of *P. falciparum* parasites, pyrimethamine-resistant polyclonal lines were established and clonal lines were isolated. *PfCCp2* gene disruption was verified in 12 isolated clones and *PfCCp3* gene disruption was verified in 6 isolated clones by a PCR assay diagnostic of an integrated locus (using primers P1 and P2 in Fig. 7; unpublished data). Further characterizations focused on two clones for each disruptant gene, termed *PfCCp2-KO* isolates D-11H and F-1D and *PfCCp3-KO* isolates H-3D and I-9C. Southern blotting analysis confirmed disrupted gene loci in all *PfCCp2-KO* and *PfCCp3-KO* clones (Fig. S2, A and C, available at <http://www.jem.org/cgi/content/full/jem.20031274/DC1>). Protein expression was not detected by Western blot analysis in gametocyte protein extracts isolated from disruptant isolates when compared with a WT NF54 iso-

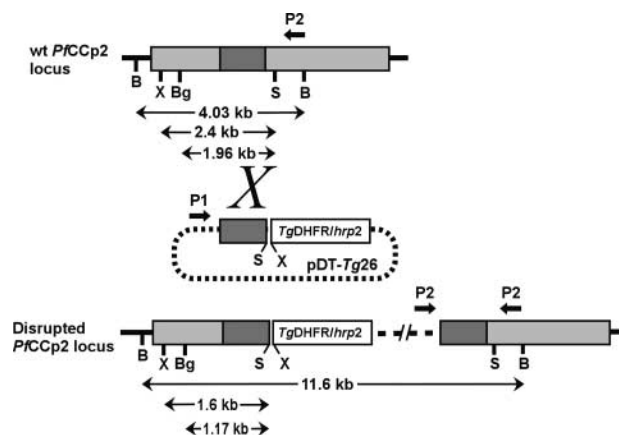


Figure 7. Schematic of the *PfCCp2* locus, the disruption plasmid construct p*PfCCp2*-KO (using the pDT-*Tg23* vector), and the organization of the *PfCCp2* locus after integration by homologous recombination. The coding region of *PfCCp2* (gray) is split into a region representing the portion homologous to the disruption plasmid (dark gray). The *T. gondii* DHFR gene and regulatory cassette are represented by a white box. Approximate location of restriction enzyme sites (B, BclI; Bg, BglII; S, SpeI; X, XbaI) and sizes of restriction digest fragments are indicated below the WT and disrupted *PfCCp2* loci (refer to Southern blot analysis shown in Fig. S2). Amplification of a PCR product using the primers P1 and P2 was diagnostic of homologous integration. The *PfCCp3* gene locus was similarly disrupted.

late control (Fig. S2, B and D). In vitro emergence assays using *PfCCp2*-KO and *PfCCp3*-KO mature gametocytes, followed by IFA using α -tubulin II or *Pfs25* labeling, indicated a normal exflagellation behavior and typical zygote and retort formation, respectively, compared with WT cultures (unpublished data). Thus, the ability to disrupt the *PfCCp2* or *PfCCp3* gene loci in asexual parasites and the abrogation of protein expression in gametocytes indicate that neither *PfCCp2* nor *PfCCp3* are essential for proliferation of asexual stages, gametocytogenesis, maturation of gametocytes in vitro, and efficient gametogenesis.

To characterize *PfCCp2*-KO and *PfCCp3*-KO phenotypes during mosquito transmission, mature gametocyte cultures of WT parasites and gene-disruptant clones were fed to *An. freeborni* mosquitoes via membrane feeding. Six independent feeding experiments for *PfCCp2*-KO cultures and two independent feeds for *PfCCp3*-KO cultures revealed a normal infection rate of mosquito midgut oocysts compared with mosquitoes fed with WT parasites (Table I). The number of oocysts per midgut was comparable in WT and gene-disruptant lines. Ultrastructural examinations of *PfCCp2*-KO (Fig. 8 A) and *PfCCp3*-KO (Fig. 8 B) oocysts indicated apparent normal differentiation, in which developed sporozoites (Fig. 8, C and D) showed no morphological differences compared with WT midgut sporozoites. However, no sporozoites were detected 19 d after feeding within or associated with salivary glands, nor within the hemocoel of mosquitoes fed with the KO lines, whereas mosquitoes fed with WT cultures exhibited salivary gland infection rates ranging from 13 to 86% (Table I). To address the fate of sporozoites, in one experiment, >50 mosquito midguts were pooled 20 d after feeding with

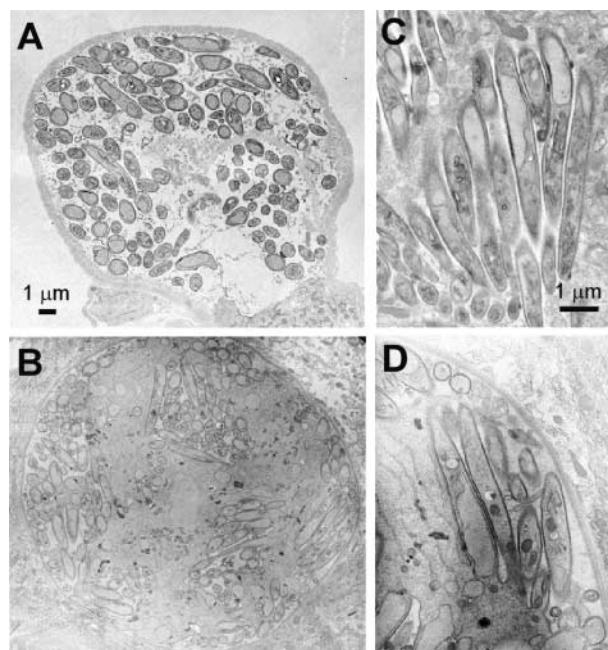


Figure 8. Development of midgut oocysts and sporozoites after mosquito membrane feeding with gene-disrupted parasites. Ultrastructural examinations 12 d after feeding show oocysts in mosquito midguts after feeding *PfCCp2*-KO clone D-11H (A) and *PfCCp3*-KO clone I-9C (B) cultures. Mature oocysts exhibit fully developed sporozoites for *PfCCp2*-KO (C) and *PfCCp3*-KO (D). Bars, 1 μ m.

PfCCp2-KO line F-1D, homogenized, and enriched for sporozoites via differential centrifugation. Specimens were screened by IFA using the mAb 2A10 recognizing the CS protein and revealed CP protein expression in sparse, intact midgut *PfCCp2*-KO sporozoites having CS protein precipitate trails indicative of motility on the glass slides (unpublished data). Thus, *PfCCp2*- and *PfCCp3*-targeted gene disruption results in a developmental blockage in the sporozoite transition from the mosquito midgut to salivary gland sporozoites.

Discussion

This study focused on the identification of novel antigens through sequence profile analysis and comparative genomics, followed by characterization of select extracellular proteins throughout the malaria parasite life cycle. Here we describe six *Plasmodium* genes unique to the Apicomplexa but having multiple domain architectures reminiscent of animal extracellular proteins. Five of these genes contain one or more LCCL domains, with four genes having orthologues in the distantly related coccidian, *C. parvum*. The conservation of multidomain architectures in orthologues across the apicomplexan clade implies that the proteins serve functions that have not diverged within specific apicomplexan lineages. Because *Plasmodium* and *Cryptosporidium* have highly diverged parasitic life strategies, it is anticipated that the multidomain adhesion proteins are not involved directly in host recognition, such as binding to

Table I. Infection Rates of Mosquito Membrane Feeds on WT and *PfCCp2* and *PfCCp3* Gene-disruptant Lines

	Oocysts	Salivary glands	
	Infectivity: infected/dissected ^a	Infectivity: infected/dissected ^b	Infectivity: percent infected
<i>PfCCp2</i> -KO			
Experiment 1			
WT	5/12	5/10	50
D-11H	3/15	0/8	—
F-1D	3/6	0/16	—
Experiment 2			
WT	12/20	4/20	20
D-11H	19/20	0/20	—
F-1D	15/20	0/20	—
Experiment 3			
WT	17/20	1/8	12.5
D-11H	20/20	0/9	—
F-1D	17/20	0/8	—
Experiment 4			
WT	oocysts present ^c	9/20	45
D-11H	oocysts present	0/12	—
Experiment 5			
WT	oocysts present	3/7	43
D-11H	oocysts present	0/13	—
F-1D	oocysts present	0/16	—
Experiment 6			
WT	oocysts present	6/7	86
D-11H	oocysts present	0/8	—
F-1D	oocysts present	0/16	—
<i>PfCCp3</i> -KO			
Experiment 6			
WT	5/12	5/10	50
H-3D	13/13	0/15	—
I-9C	16/16	0/11	—
Experiment 2			
WT	13/13	4/9	44
H-3D	6/7	0/14	—
I-9C	5/5	0/16	—

^aNumber of infected mosquitoes with one or more oocysts per total number of mosquitoes dissected.

^bNumber of infected mosquitoes with salivary gland sporozoites present per total number of mosquitoes dissected.

^cIn these experiments, it was determined if transmission progressed to the oocyst stage, and the remaining mosquitoes were saved for salivary gland determinations.

host cell surface proteins or interacting with components of the host immune system. Otherwise, it would be necessary to propose that recognition of a specific host molecule is conserved across the apicomplexan clade. It is more likely that a proposed host ligand is “generic,” such as the sugar moieties of heparin sulfate or other proteoglycans within host cell surfaces or extracellular matrices. This proposal is supported by the presence of multiple putative polysaccha-

ride-binding domains in the architectures of the family members. This is also consistent with the observed mutant phenotype in which *PfCCp2* and *PfCCp3*-KO parasites fail to progress to the salivary glands, via possible disruption of interactions with host glycoproteins mediating this process. On the other hand, an alternative explanation might be that at least some of the proteins were recruited to serve an “ancient” parasite-specific cellular function, such as partici-

pation in a stage-specific aspect of the parasitophorous vacuole, formation of structures associated with the parasite pellicule, or serving in the formation of an extracellular matrix surrounding one or more emerged parasite stages. Either of the two proposed models must take into account a role for the multiple putative polysaccharide-binding domains within the LCCL domain proteins. It is likely that the expression stage specificity is conserved across genera and support for CCp function might ultimately be provided by the study of life cycle stage of expression and localization in additional apicomplexans, such as *Cryptosporidium* and *Toxoplasma*.

Transcript expression studies show abundant gametocyte-specific expression for five of the six multidomain adhesion proteins. Protein expression and immunolocalization studies for three selected proteins, *PfCCp1*, *PfCCp2*, and *PfCCp3*, indicate that the proteins colocalize and are released during gametogenesis and remain associated with gamete aggregates. Gametocyte-specific expression of *PfCCp* proteins is supported by high throughput mass spectrometry proteomic analysis of *P. yoelii* rodent malaria sexual stage parasites (35), as well as a recent study showing gametocyte-specific transcript and protein expression of *PSLAP/PfCCp3* in *P. falciparum* (3). In the latter study, cellular localization revealed submembranous expression or secretion to the parasitophorous vacuole and erythrocyte cytoplasm of mature gametocytes. This localization pattern is similar to that observed in our indirect IFA and immunoelectron microscopy studies.

To begin to address function of the LCCL domain family members, we have disrupted the *PfCCp2* and *PfCCp3* gene loci and have shown that neither gene is essential for asexual proliferation or required for efficient gametocytogenesis. Despite abundant gametocyte stage expression in WT parasites, gene-disruptant lines formed gametes efficiently and, after membrane feeds to anophelene mosquitoes, formed midgut wall oocysts with efficiency similar to WT. Oocysts mature normally and intact sporozoites are released, but a block in transmission occurred during the mature midgut oocyst to salivary gland sporozoite transition. Hemocoel sporozoites were not detected, nor were sporozoites adhering to salivary glands. The fate of the gene-disruptant sporozoites is not yet known, with one possibility being that the sporozoites remain and subsequently degrade within the mosquito midgut. It is thus far not possible to interpret the discrepancy between the prominent *PfCCp* transcript and protein expression observed in gametocyte stages and the manifestation of a phenotype in *PfCCp2* and *PfCCp3* gene disruptants during late stages of midgut oocyst development. It is unlikely that the phenotype is due to an "epigenetic artifact" because it would require proposing that a similar epigenetic phenotype has occurred after disruption of either of the genetically unlinked genes, *PfCCp2* and *PfCCp3*. The oocyst stage phenotype may either be linked in an as yet unknown fashion to protein function in gametocytes or might be due to abrogation of undetected low level sporozoite stage pro-

tein expression. The latter hypothesis is supported by recent description of a *CpCCP1/2* homologue expressed in *Cryptosporidium* sporozoites (36, 37). *CpCCP1/2* protein also localized to the parasitophorous vacuole in 72-h infected HCT-8 cells, thus drawing a parallel with *Plasmodium* gametocyte cellular localization in this study and providing support that the LCCL domain family members serve roles in multiple parasite stages.

Targeted gene disruption of *PbSR* (*PbCCp3/PbSLAP*) in the rodent malaria model, *P. berghei*, also results in a block in late stage oocyst maturation (4) and the phenotype is superficially similar to *PfCCp2*-KO and *PfCCp3*-KO. In contrast to the *PbSR* study (4), we were unable to detect *PfCCp3* protein expression in sporozoites by IFA and Western blot assays using mouse sera directed against recombinant protein corresponding to the tandem SR domains. Whereas Claudianos et al. (4) describe 40- and 60-kD proteins by Western blot and immunolocalization in sporozoites using SR antipeptide sera, we detect a protein with the expected full-length molecular weight of 150 kD in *P. falciparum* gametocyte protein extracts, although we have not addressed possible proteolytic maturation of the protein during gamete emergence. The discrepancy in the two studies might be due to either sporozoite-specific processing resulting in a truncated protein contaminating protease activity in the sporozoite preparations, or nonspecific reactivity of one or more antibody reagents. Similar to our observations, Delrieu et al. (3) show that *PSLAP/PfCCp3* is expressed in gametocytes and if gametocyte expression holds for *P. berghei*, it would suggest that expression of multiple *PfCCp* proteins are essential for sporozoite development, whereas expression in gametocytes is marked but not essential for in vitro development.

Transmission-blocking vaccines target sexual phase parasite antigens, thereby relying on human antibodies to inhibit parasite development within the mosquito host (38–40). The sexual stage expression and extracellular localization of *PfCCp1*, *PfCCp2*, and *PfCCp3* make them potential vaccine candidates, and targeted gene disruption of *PfCCp2* and *PbSR/PfCCp3* further demonstrate that these highly conserved apicomplexan proteins are essential for *P. falciparum* development in the mosquito vector. *PfCCp* transmission-blocking assays are currently being pursued in our laboratory to investigate *PfCCps* as candidates for study as subunits of a transmission-blocking vaccine.

We thank Heather Eisen, Darrow Deluca, and Amina Kurtovic for technical assistance. We also thank Dr. Elizabeth Nardin for kindly providing the mAb 2A10, and David Keister, Olga Muratova, and Andre Laughinghouse for mosquito and parasite material, mosquito rearing, and mosquito feeds. Drs. Kirk Deitsch and Carl Nathan are thanked for critically reviewing the manuscript.

This work was supported by the Niarchos Foundation. The Department of Microbiology and Immunology at Weill Medical College of Cornell University acknowledges the support of the William Randolph Hearst Foundation.

Submitted: 28 July 2003

Accepted: 12 April 2004

References

- Gardner, M.J., N. Hall, E. Fung, O. White, M. Berriman, R.W. Hyman, J.M. Carlton, A. Pain, K.E. Nelson, S. Bowman, et al. 2002. Genome sequence of the human malaria parasite *Plasmodium falciparum*. *Nature*. 419:498–511.
- Carlton, J.M., S.V. Angiuoli, B.B. Suh, T.W. Kooij, M. Perteza, J.C. Silva, M.D. Ermolaeva, J.E. Allen, J.D. Selengut, H.L. Koo, et al. 2002. Genome sequence and comparative analysis of the model rodent malaria parasite *Plasmodium yoelii yoelii*. *Nature*. 419:512–519.
- Delrieu, I., C.C. Waller, M.M. Mota, M. Grainger, J. Langhorne, and A.A. Holder. 2001. PSLAP, a protein with multiple adhesive motifs, is expressed in *Plasmodium falciparum* gametocytes. *Mol. Biochem. Parasitol.* 121:11–20.
- Claudianos, C., J.T. Dessens, H.E. Trueman, M. Arai, J. Mendoza, G.A. Butcher, T. Crompton, and R.E. Sinden. 2002. A malaria scavenger receptor-like protein essential for parasite development. *Mol. Microbiol.* 45:1473–1484.
- Altschul, S.F., T.L. Madden, A.A. Schaffer, J. Zhang, Z. Zhang, W. Miller, and D.J. Lipman. 1997. Gapped BLAST and PSI-BLAST: a new generation of protein database search programs. *Nucleic Acids Res.* 25:3389–3402.
- Notredame, C., D.G. Higgins, and J. Heringa. 2000. T-Coffee: a novel method for fast and accurate multiple sequence alignment. *J. Mol. Biol.* 302:205–217.
- Rost, B. 1996. PHD: predicting one-dimensional protein structure by profile-based neural networks. *Methods Enzymol.* 266:525–539.
- Kumar, S., K. Tamura, I.B. Jakobsen, and M. Nei. 2001. MEGA2: molecular evolutionary genetics analysis software. *Bioinformatics.* 17:1244–1245.
- Felsenstein, J. 1996. Inferring phylogenies from protein sequences by parsimony, distance, and likelihood methods. *Methods Enzymol.* 266:418–427.
- Hasegawa, M., H. Kishino, and N. Saitou. 1991. On the maximum likelihood method of molecular phylogenies. *J. Mol. Evol.* 32:443–445.
- Nielson, H., J. Engelbrecht, S. Brunak, and G. von Heijne. 2001. Identification of prokaryotic and eukaryotic signal peptides and prediction of their cleavage sites. *Protein Eng.* 10:1–6.
- Krogh, A., B. Larsson, G. von Heijne, and E.L. Sonnhammer. 2001. Predicting transmembrane protein topology with a hidden Markov model: application to complete genomes. *J. Mol. Biol.* 305:567–580.
- Ifediba, T., and J.P. Vanderberg. 1981. Complete *in vitro* maturation of *P. falciparum* gametocytes. *Nature*. 294:364–366.
- Templeton, T.J., D.B. Keister, O. Muratova, J.L. Procter, and D.C. Kaslow. 1998. Adherence of erythrocytes during exflagellation of *Plasmodium falciparum* microgametes is dependent on erythrocyte surface sialic acid and glycoporphins. *J. Exp. Med.* 187:1599–1609.
- Bishop, A., and B.M. Gilchrist. 1946. Experiments upon the feeding of *Aedes aegypti* through animal membranes with a view to applying this method to the chemotherapy of malaria. *Parasitology.* 37:85–100.
- Nardin, E.H., V. Nussenzweig, R.S. Nussenzweig, W.E. Collins, K.T. Harinasuta, P. Tapchaisri, and Y. Chomcham. 1982. Circumsporozoite proteins of human malaria parasites *Plasmodium falciparum* and *Plasmodium vivax*. *J. Exp. Med.* 156:20–30.
- Rawling, D.J., and D.C. Kaslow. 1992. A novel 40-kDa membrane-associated EF-hand calcium binding protein in *Plasmodium falciparum*. *J. Biol. Chem.* 267:3976–3982.
- Templeton, T.J., H. Fujioka, M. Aikawa, K.C. Parker, and D.C. Kaslow. 1997. *Plasmodium falciparum* Pfs40, renamed Pfs39, is localized to an intracellular membrane-bound compartment and is not sexual stage-specific. *Mol. Biochem. Parasitol.* 90:359–365.
- Rawlings, D.J., H. Fujioka, M. Fried, D.B. Keister, M. Aikawa, and D.C. Kaslow. 1992. Alpha-tubulin II is a male-specific protein in *Plasmodium falciparum*. *Mol. Biochem. Parasitol.* 56:239–250.
- Kaslow, D.C., I.A. Quakyi, C. Syin, M.G. Raum, D.B. Keister, J.E. Coligan, T.F. McCutchan, and L.H. Miller. 1988. A vaccine candidate from the sexual stage of human malaria that contains EGF-like domains. *Nature*. 333:74–76.
- Kaslow, D.C., I.C. Bathurst, T. Lensen, T. Ponnudurai, P.J. Barr, and D.B. Keister. 1994. *Saccharomyces cerevisiae* recombinant Pfs25 absorbed to alum elicits antibodies that block transmission of *Plasmodium falciparum*. *Infect. Immun.* 62:5576–5580.
- Wu, Y., L.A. Kirkman, and T.E. Wellems. 1996. Transformation of *Plasmodium falciparum* malaria parasites by homologous integration of plasmids that confer resistance to pyrimethamine. *Proc. Natl. Acad. Sci. USA.* 93:1130–1134.
- Templeton, T.J., D.C. Kaslow, and D.A. Fidock. 2000. Developmental arrest of the human malaria parasite *Plasmodium falciparum* within the mosquito midgut via *CTRP* gene disruption. *Mol. Microbiol.* 36:1–9.
- Deitsch, K.W., C. Driskill, and T. Wellems. 2001. Transformation of malaria parasites by the spontaneous uptake and expression of DNA from human erythrocytes. *Nucleic Acids Res.* 29:850–853.
- Goodyer, I.D., and T.F. Taraschi. 1997. *Plasmodium falciparum*: a simple, rapid method for detecting parasite clones in microtiter plates. *Exp. Parasitol.* 86:158–160.
- Baumgartner, S., K. Hofmann, R. Chiquet-Ehrismann, and P. Bucher. 1998. The discoidin domain family revisited: new members from prokaryotes and a homology-based fold prediction. *Protein Sci.* 7:1626–1631.
- Ponting, C.P., and R.B. Russell. 2000. Identification of distant homologues of fibroblast growth factors suggests a common ancestor for all beta-trefoil proteins. *J. Mol. Biol.* 302:1041–1047.
- Trexler, M., L. Banyai, and L. Patthy. 2000. The LCCL module. *Eur. J. Biochem.* 267:5751–5757.
- Missler, M., R. Fernandez-Chacon, and T.C. Sudhof. 1998. The making of neurexins. *J. Neurochem.* 71:1339–1347.
- Bork, P. 1992. The modular architecture of vertebrate collagens. *FEBS Lett.* 307:49–54.
- Doolittle, R.F. 1992. A detailed consideration of a principal domain of vertebrate fibrinogen and its relatives. *Protein Sci.* 1:1563–1577.
- Spraggon, G., S.J. Everse, and R.F. Doolittle. 1997. Crystal structures of fragment D from human fibrinogen and its crosslinked counterpart from fibrin. *Nature*. 389:455–462.
- Lu, J., and Y. Le. 1998. Ficolins and the fibrinogen-like domain. *Immunobiology.* 199:190–199.
- Tsuji, S., J. Uehori, M. Matsumoto, Y. Suzuki, A. Matsuhisa, K. Toyoshima, and T. Seya. 2001. Human intelectin is a novel soluble lectin that recognizes galactofuranose in carbohydrate chains of bacterial cell wall. *J. Biol. Chem.* 276:23456–23463.
- Lasonder, E., Y. Ishihama, J.S. Andersen, A.M. Vermunt, A. Pain, R.W. Sauerwein, W.M. Eling, N. Hall, A.P. Waters,

- H.G. Stunnenberg, et al. 2002. Analysis of the *Plasmodium falciparum* proteome by high-accuracy mass spectrometry. *Nature*. 419:537–542.
36. Tosini, F., S. Caccio, A. Tamburrini, G. La Rosa, and E. Pozio. 1999. Identification and characterization of three antigenic proteins from *Cryptosporidium parvum* sporozoites using a DNA library expressing poly-histidine tagged peptides. *Int. J. Parasitol.* 29:1925–1933.
37. Tosini, F., A. Agnoli, R. Mele, M.A.G. Moralez, and E. Pozio. 2004. A new modular protein of *Cryptosporidium parvum*, with ricin B and LCCL domains, expressed in the sporozoite invasive stage. *Mol. Biochem. Parasitol.* 134:137–147.
38. Carter, R., K.N. Mendis, L.H. Miller, L. Molineaux, and A. Saul. 2000. Malaria transmission-blocking vaccines—how can their development be supported? *Nat. Med.* 6:241–244.
39. Carter, R. 2001. Transmission blocking malaria vaccines. *Vaccine*. 19:2309–2314.
40. Kaslow, D.C. 2002. Transmission-blocking vaccines. *Chem. Immunol.* 80:287–307.